

# A Novel Optimized Neural Network Model for Ink Selection in Printed Electronics

Alagusundari Narayanan<sup>1\*</sup> and Dr. Sivakumari Subramania Pillai<sup>2</sup>

<sup>1,2</sup>Department of Computer Science and Engineering, School of Engineering, Avinashilingam Institute for Home Science and Higher Education for Women, Coimbatore, Tamilnadu, India.

\*Correspondence: Alagusundari Narayanan: nalagusundari43@gmail.com

**ABSTRACT-** The field of Printed Electronics (PE) is experiencing significant growth in the industrial sector and generating considerable interest across various industries due to its ability to produce intricate components. The functionality of printed electronic products heavily relies on the utilization of conductive ink during the printing process, which plays a vital role in developing flexible electronic circuits and improving the communicative functionalities of objects. Selecting the right ink for printing is crucial to meet consumer requirements. However, the conventional approach to this process has been manual, labor-intensive, and time-consuming, relying on the expertise of designers. This paper presents an automated ink selection model for printed circuits. This novel method has been incorporated with Multilayer Perceptron Neural Network (MLPNN) and Particle Swarm Optimization (PSO), named PSO-MLPNN. A dataset containing material features is generated by gathering information from both literature and experimental observations. To ensure uniformity, the data undergoes preprocessing using the min-max method, which scales all features to a standardized range between 0 and 1. A four-layer MLPNN is constructed to choose the most suitable ink. The network is trained with the PSO algorithm. The bias and weight values of MLPNN are tuned using the PSO algorithm to attain high accuracy. The computed findings confirm that the ink selection is highly effective and more accurate when compared to both the standard MLPNN.

**Keywords:** Conductive ink, Ink selection, Multilayer perceptron, Printed Electronics, Particle swarm optimization.

## ARTICLE INFORMATION

**Author(s):** Alagusundari Narayanan & Dr. Sivakumari Subramania Pillai;

**Received:** 11/09/23; **Accepted:** 22/11/23; **Published:** 02/12/23

**E- ISSN:** 2347-470X

**Paper Id:** IJEER230731

**Citation:** 10.37391/IJEER.110430

**Webpage-link:**

<https://ijeer.forexjournal.co.in/archive/volume-11/ijeer-110430.html>



**Publisher's Note:** FOREX Publication stays neutral with regard to jurisdictional claims in Published maps and institutional affiliations.

## 1. INTRODUCTION

For over six decades, electronic devices have been manufactured through a complex series of photo-lithographic and chemical processes, resulting in the creation of electronic circuits on materials like silicon or semiconductors. Printed Electronics (PE) offers an alternative approach to manufacturing electronic circuits. It utilizes standard graphic arts printing techniques to create diverse electronic devices by forming conductive traces on a typically organic and flexible substrate. The market for printed sensors on flexible substrate is expanding rapidly, with estimates suggesting it will reach \$7.6 billion by 2027 [1], [2]. PE possesses unique attributes, including novel physical forms (flexible, stretchable, ultra-thin), compatibility with various substrates (paper, plastic, textile), and cost-effective mass production. These characteristics present opportunities for numerous applications in consumer electronics, pharmaceuticals, packaging, touchscreen displays, Radio Frequency Identification (RFID)

tags, electronics, textiles, and other sectors [3].

Conductive ink is a substance that can be printed, and processed to enable the flow of electricity. It serves as a foundational component in PE, forming the essential structure of circuit boards and devices. Conductive inks are responsible for creating low-resistance circuit interconnects, antennas, contact electrodes within transistors, and other integrated functionalities [4]. The significance of conductive inks in the production of PE devices has gained significant recognition in recent years. Different types of inks are utilized for printing applications. The quality of these inks varies based on their intended applications, and this variation significantly impacts the final product. Choosing the correct ink is a critical prerequisite for achieving suitable results [5]. Manipulating the material properties can influence the quality of the product. In this context, this study focuses on the crucial step of selecting the appropriate conductive ink for card printing. If the ink selection is not done correctly, the printed cards may exhibit flaws, adversely affecting the overall quality and appearance. Hence, the development of an automated technique for ink selection in printing is imperative.

The PE technique involves numerous process variables that will directly influence the product quality. Accomplishing optimal results requires interdisciplinary knowledge encompassing factors such as material characteristics, substrates, and more. Characteristically, these parameters are determined using physics-based approaches, which can be challenging, time-consuming, and prone to errors. To address the constraints of physics-based approaches and enhance the

final product's quality, Machine Learning (ML) models have been adopted in PE. In previous studies, ML methods have been applied by researchers to suggest design features [6], enhancing the overall printing process [7], and optimizing the ejection of drops [8]. Conductive ink significantly influences the quality of final products. However, an automated system for conductive ink selection has not yet been established. Therefore, the creation of an automated system for conductive ink selection is essential to improve the final product's quality. This study is chiefly motivated by the objective of developing an automated system that utilizes ML and PSO algorithms to choose the most appropriate ink for printing applications based on the input values. The principal contributions of this study are outlined as follows:

- (i) A four-layer Multilayer Perceptron Neural Network (MLPNN) is built to select ink for PE.
- (ii) Weight and bias values are optimized using the PSO procedure.
- (iii) To determine the optimal network configuration for printing applications, the developed system's effectiveness is evaluated by varying the counts of hidden layers, hidden neurons, as well as the training and testing samples.
- (iv) Extensive experiments are carried out using real-world data to assess the effectiveness of the developed system. The empirical outcomes indicate that the PSO-MLPNN is capable of accurately selecting ink for printing applications.

The organization of the paper is as follows. *Section 2* offers a concise overview of earlier approaches. *Section 3* outlines the ink selection system that is developed. *Section 4* overviews the outcomes of the performance evaluation. Lastly, *section 5* gives the conclusion for this study.

## 2. LITERATURE SURVEY

This section provides a brief overview of the use of machine learning techniques in various aspects of PE. Matsuhisa et al. [3] provided a detail about elastic conductors for textile applications. Huang et al. [4] introduced graphene laminate for printed radio frequency applications.

Li et al. [5] presented a multi-color display system using phot-patterning and transfer printing. Yao et al. [6] introduced a hybrid technique that combines Hierarchical Clustering (HC) and Support Vector Machine (SVM) for design feature recommendation. HC was employed to categorize design features, while SVM enhanced the HC outcomes to identify recommended design features. This technique proved useful in helping new designers identify suitable design features for printing applications.

Brishty et al. [8] explored the potential of machine learning algorithms in categorizing ink and printed parameters based on the jetting regime. Three algorithms, namely K-nearest Neighbour (KNN), Neural Network (NN), and Decision Tree (DT), were utilized for ink classification. The NN classifier outperformed KNN and DT.

Vahabli & Rahmati [9] used the Radial Basis Function Neural Network (RBFNN) to enhance the quality of printed circuits.

Ansari et al. [11] presented an interesting method for selecting inks for spectral reproduction. This approach involved taking a painting and utilizing mixed-integer programming to detect optimal inks for spectral reproduction.

Nagasawa et al. [12] introduced a method for determining skin color and translucency using the line spread function and NN. This method generated multi-layered color patches of human skin, computed the line spread function, and employed NN to estimate the layout.

Wu & Xu [13] employed an NN model to predict drop speed and ink volume. The model was trained using input features such as rise time, voltage, and pulse duration to carry out accurate prediction. Rama et al. [14] discussed the preparation of conductive inks and their application in PE and flexible electronics. The superiority of chemical methods for synthesizing Ag-ink was demonstrated.

Jansson et al. [15] analyzed the printing effectiveness of metal conducting layers on dissimilar paper-based substrates utilizing flexography as well as scanning electron microscopy. The re-pulpability capability of the substrates was also assessed accordingly.

## 3. PROPOSED METHODOLOGY

The general structure of the model suggested is depicted in *figure 1*. The key elements in the suggested model are data collection, data division, training, and testing. The data collection unit collects the required input and output variables.

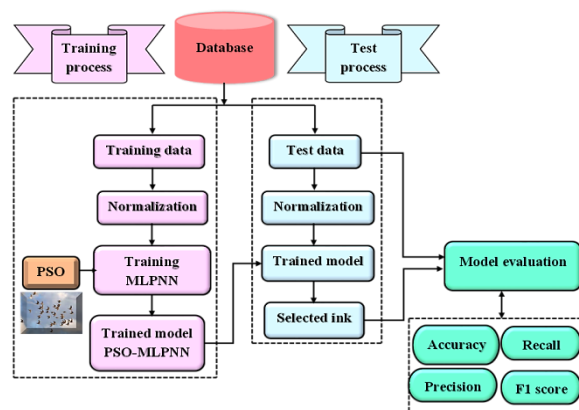


**Figure 1:** Workflow of the proposed system for printing applications

The data division unit then separates the data into in-sample and out-sample datasets, which are used for training and testing purposes, correspondingly. The training unit is responsible for training the MLPNN to establish the association among input and output parameters. Finally, the testing unit assesses the trained ink.

### 3.1. Data gathering

Data gathering is a crucial step in modeling an Artificial Neural Network (ANN) for printing applications. The data collection phase in this study encompassed two main aspects: material properties and conductive inks. The MLPNN utilizes the material characteristics to determine the appropriate ink for

printing. The study focused on three types of conductive inks: carbon, copper, and silver inks. To ensure successful printing, several key material characteristics are considered, including product life, quality, handling and usage, grammage, caliper, brightness, tear resistance, and moisture content. Three conductive inks are chosen as targets such as Carbon, Copper, and Silver inks. These properties are listed in Table 1.

### 3.2. Data division

Data division involves separating the data into two distinct sets: in-sample and out-sample data. The training set comprises 80% of the data and is utilized for training the model, whereas the testing set comprises 20% of the data and is utilized for evaluating the model's performance.

**Table 1: Input variables and targets used in this work**

Input Features								Targets
Product life (1-5)	Product Quality (1-5)	Product usage and handling (1-5)	Grammage (gsm)	Caliper/Thickness (mm)	Brightness (%)	Tear resistance (mN)	Moisture content (g/m <sup>2</sup> )	Conductive ink
2	2	3	78	103	93	63	41	Carbon Ink
5	5	5	101	112	95	68	40	Silver ink
4	2	1	83	109	92	65	42	Silver ink
3	3	5	200	250	93	101	18	Silver ink
4	2	1	110	108	94	72	20	Carbon ink
3	3	4	280	261	92	151	19	Silver ink
3	3	2	98	115	93	121	38	Carbon ink
4	2	4	250	255	92	131	39	Silver ink
4	2	3	68	115	89	125	37	Carbon ink
3	2	4	68	115	89	125	36	Carbon ink
3	2	2	62	110	91	84	35	Carbon ink
3	5	3	170	100	90	78	40	Silver Ink
3	2	3	180	190	50	56	43	Carbon ink
3	2	4	100	105	80	86	46	Copper Ink
3	2	2	80	102	50	83	41	Copper ink
2	3	2	100	110	60	92	36	Carbon ink
2	2	2	160	171	65	87	38	Carbon ink
3	4	3	200	250	98	142	12	Silver ink
2	4	2	190	208	96	125	15	Silver ink
2	3	2	100	132	94	115	12	Copper ink

### 3.3. Data normalization

Due to the sensitivity of ANN input data, the input features and target values are scaled to a range of 0 to 1 via data normalization. This normalization is achieved using the min-max method, as described in [9]. The normalization can be mathematically represented as follows:

$$x_{norm} = \frac{x - \min(x)}{\max(x) - \min(x)} \quad (1)$$

Where  $x$  and  $x_{norm}$  are the input and normalized values, respectively. Also,  $\min$  and  $\max$  are minimum and maximum values, correspondingly.

### 3.4. Particles swarm optimization

In this study, an MLPNN is designed with an input layer with  $m$  input neurons, two hidden layers with 12 hidden neurons in each layer, and an output layer with three neurons. The weights and bias values are optimized using the PSO algorithm.

PSO is a population-based algorithm, presented by Eberhart & Kennedy [10]. It is widely used for fine-tuning the parameters of neural networks [16] [17] [18].

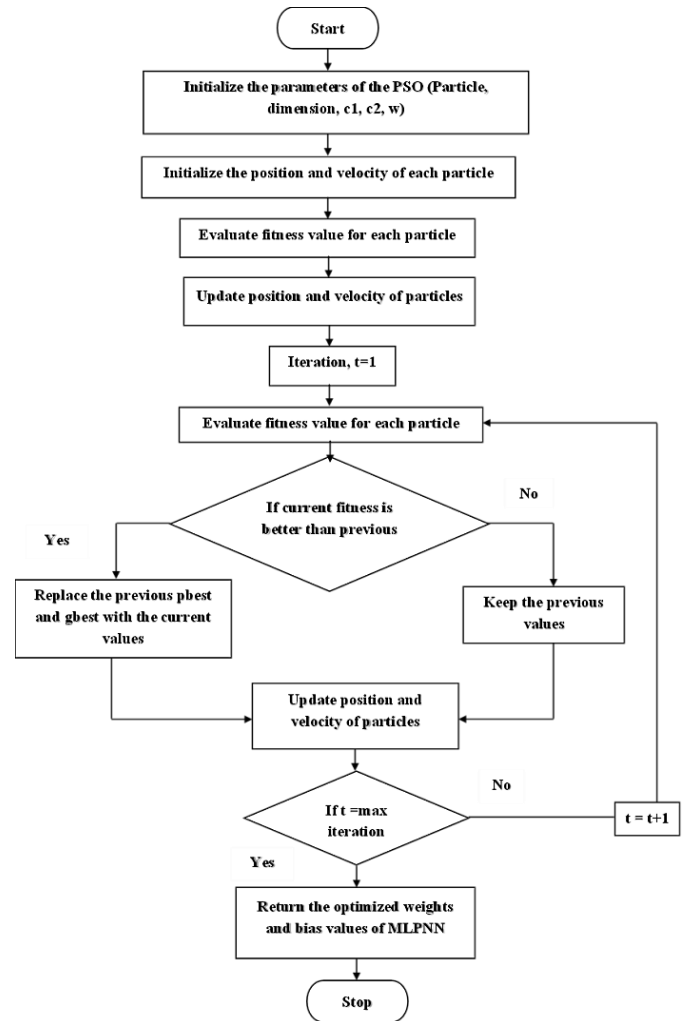


**Figure 2: Flowchart of the PSO-MLPNN for ink selection**

In this study, the PSO is adopted to tune the parameters of the MLPNN because of its capacity to adapt, flexibility, faster convergence, fewer control parameters, and superior ability to balance both exploration and exploitation.

PSO is based on the imitation of the communal behavior of birds within a group. Let the population size,  $M$ , and dimensional size of the problem,  $D$ . Each particle is a possible solution, characterized by a velocity of  $V_n = [V_{n,1}, V_{n,2}, \dots, V_{n,D}]$  and a position vector of  $X_n = [X_{n,1}, X_{n,2}, \dots, X_{n,D}]$ , where,  $n=1, 2, \dots, M$ . During the  $t^{th}$  iteration of the searching procedure,

the new velocity  $V_{n,d}^{t+1}$  of all n-th particles in any dimension,  $D$  is varied based on the equivalent dimensional elements of the personal best position  $X_{n,d}^{pbest,t}$  (self-cognitive component) and global best position  $G_{n,d}^{best,t}$  (social component) as below:

$$V_{n,d}^{t+1} = \omega V_{n,d}^t + c_1 r_1 (X_{n,d}^{pbest,t} - X_{n,d}^t) + c_2 r_2 (G_{n,d}^{best,t} - X_{n,d}^t) \quad (2)$$

where  $\omega$ -inertia weight,  $c1$  and  $c2$ -acceleration coefficients,  $r1$ ,  $r2$  -random numbers [0,1]. The upcoming position of all the n-th particles in all dimensions is updated as:

$$X_{n,d}^{t+1} = V_{n,d}^{t+1} + X_{n,d}^t \quad (3)$$

The fitness values of all the  $n^{th}$  particles are calculated and equated with those of the personal best position and global best positions. Both will be restructured if the last solution is greater. The search procedure is continued until the predefined criteria are met.

In this study, the PSO procedure is utilized for optimizing the MLPNN parameters. The flowchart of the PSO-MLPNN designed for ink selection is shown in *figure 2*. The necessary algorithmic steps of the proposed system are as follows:

*Step 1:* Read input data and target.

*Step 2:* Preprocess the collected data using *equation (1)*.

*Step 3:* Divide the preprocessed data into train and test samples.

*Step 4:* Design an MLPNN and initialize the parameters.

*Step 5:* Initialize the parameters of the PSO algorithm.

*Step 6:* Optimize the MLPNN parameters using PSO.

*Step 7:* Test the MLPNN with test data.

*Step 8:* Compare the classified output with the test target.

## 4. EMPIRICAL STUDY

In this section, a comprehensive overview of the numerical outcomes obtained from the ink selection system for printing applications. The presented system has been successfully implemented using the MATLAB 2022a platform.

### 4.1. Performance metrics

The effectiveness of the designed system is assessed through the calculation of different parameters like accuracy, recall, precision, and F1 score. The system's viability is analyzed using a confusion matrix, which consists of four values: True positive (TP) is when a system appropriately categorizes the positive classes, True Negative (TN) corresponds to the class when the system appropriately categorizes the negative classes when the system incorrectly classifies the positive classes, the outcome is a False Positive (FP), and when the system incorrectly classifies negative class, it generates a False Negative (FN).

In this work, multiclass classification is considered. The TP classes are the labels for which the calculations are being

carried out and the negative classes are the remaining labels. The metrics are given below:

$$Accuracy = \frac{TP+TN}{TP+TN+FP+FN} \quad (4)$$

$$Precision = \frac{TP}{TP+FP} \quad (5)$$

$$Recall = \frac{TP}{TP+FN} \quad (6)$$

$$F1 - score = 2 X \frac{Precision \times Recall}{Precision+Recall} \quad (7)$$

### 4.2. Performance analysis

Through a series of experiments, the essential parameters for designing PSO- MLPNN were determined. Various tests were carried out to establish the optimal PSO-MLPNN structure. *Table 2* lists the simulation variables used in these experiments.

**Table 2: MLPNN parameters**

S.No.	Parameters	Value
1.	No. of input neurons	8
2.	No. of hidden layers	1 to 4
3.	No. of hidden neurons in the hidden layer	10 to 15
4.	No. of output neurons	3
5.	Hidden layer activation function	Sigmoidal
6.	Output layer activation function	Linear
7.	Epoch	1000
8.	Momentum	0.01
9.	Training algorithm	PSO and LM

The effectiveness of the PSO-MLPNN was evaluated through three different scenarios:

**Experiment 1:** The performance of the system was analyzed by varying the count of hidden neurons.

**Experiment 2:** The efficacy of the system was evaluated by changing the count of hidden layers.

**Experiment 3:** The effectiveness of the system was assessed by varying the count of training and testing data.

The MLPNN was built with input, hidden, and output layers. The hidden layer utilized a sigmoidal activation function, while the output layer employed a linear activation function. During the training phase, the MLPNN was trained separately using PSO and LM procedures to augment its parameters. In the testing phase, the performance of the trained network was assessed using test data. All experiments were repeated several times and mean values were reported.

#### 4.2.1. Experiment 1

In the first experiment, the input data was divided into two sets: 80% of the samples were assigned for training, whereas the leftover 20% were utilized for testing. The range of hidden layers explored was from 10 to 15. The developed MLPNN was separately trained using LM and PSO algorithms. The outcomes of the first experiment are summarized in *Table 3*. It



is observed from *table 3* that the PSO-MLPNN provided better performance than MLPNN for all cases. Upon examining *table 3*, it is evident that the MLPNN attained the lowest accuracy of 70.01%, recall of 82.50%, precision of 75.01%, and F1-Score of 78.57% when using a single hidden layer with 10 hidden neurons. However, the developed PSO-MLPNN yielded higher performance with an accuracy of 88.19%, recall of 88.57%, precision of 76.68%, and F1-Score of 83.33% compared to the MLPNN approach.

An increase in the number of neurons from 10 to 12 ensued in an improvement in the classification rate. With 12 hidden neurons, both the MLPNN and PSO-MLPNN exhibited exceptional performance, reaching accuracy of 86.67% and 94.48%, recall of 95% and 96%, precision of 86.36% and 88.42%, and F1-score of 90.48% and 92.05%, respectively. However, if the number of neurons increases further to 13, 14, or 15, the classification rate is decreased. For a single hidden layer with 15 hidden neurons, the MLPNN achieved an accuracy of 80%, while PSO-MLPNN yielded an accuracy of 90.86%. This comparison indicates that the system with 12 hidden neurons performed the best. As a result, 12 hidden neurons were chosen as the optimal configuration. *Figure 3* provides a graphical representation of the data presented in *Table 3*. Notably, the system attained the lowest accuracy for 10 hidden neurons. Increasing the number of neurons beyond 12 led to unstable performance. So, 12 hidden neurons were selected to ensure improved performance.

**Table 3: Efficacy comparison between MLPNN and PSO-MLPNN for dissimilar numbers of hidden neurons**

No. of hidden neurons	Models	Accuracy (%)	Recall (%)	Precision (%)	F1 score (%)
10	MLPNN	70.01	82.5	75.01	78.57
	PSO-MLPNN	88.19	88.57	78.68	83.33
11	MLPNN	73.33	82.5	78.57	80.49
	PSO-MLPNN	89.14	89.71	80.1	84.64
12	MLPNN	86.67	95	86.36	90.48
	PSO-MLPNN	94.48	96	88.42	92.05
13	MLPNN	81.67	90	83.72	86.75
	PSO-MLPNN	92.19	94.29	84.18	88.95
14	MLPNN	85	87.5	89.74	88.61
	PSO-MLPNN	91.43	93.14	83.16	87.87
15	MLPNN	80	85	85	85
	PSO-MLPNN	90.86	92.57	82.23	87.1

#### 4.2.2. Experiment 2

In the second phase of the experiment, the hidden layers were varied from 1 to 4, while the hidden neurons were fixed at 12. The performance of the developed system was evaluated for each configuration, and outcomes are reported in *table 4*. According to *table 4*, both the MLPNN and PSO-MLPNN

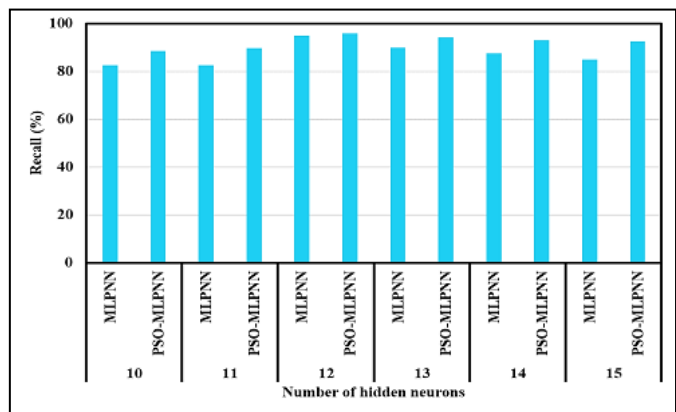
achieved their highest accuracy, recall, and F1-score values were 91.67% and 96.38%, 95% and 97.71%, 92.68%, and F1-score of 93.83% and 94.74%, respectively, when using two hidden layers with 12 hidden neurons. However, increasing the number of hidden layers to 3 or 4 resulted in a degradation of the system's effectiveness. Consequently, it shall be fixed that the optimal number of hidden layers for the MLPNN is 2. The pictorial delineation of *table 4* is given in *figure 4*.

**Table 4. Performance comparison between MLPNN and PSO-MLPNN for different numbers of hidden layers**

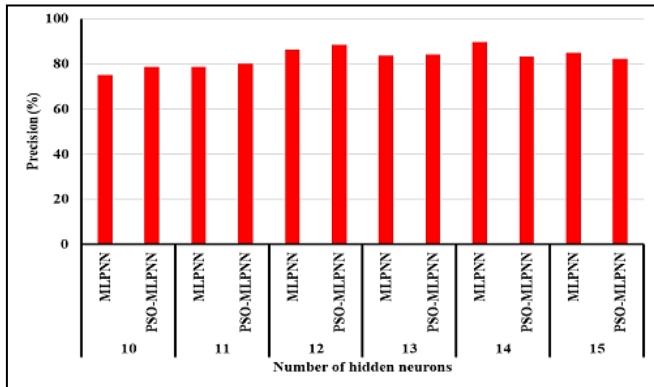
No. of hidden neurons	Models	Accuracy (%)	Recall (%)	Precision (%)	F1 score (%)
1	MLPNN	86.67	95	86.36	90.48
	PSO-MLPNN	94.48	96	88.42	92.05
2	MLPNN	91.67	95	92.68	93.83
	PSO-MLPNN	96.38	97.71	91.94	94.74
3	MLPNN	80	90	81.82	85.71
	PSO-MLPNN	92.38	93.71	84.97	89.13
4	MLPNN	73.33	80	80	80
	PSO-MLPNN	90.48	92	81.73	86.56



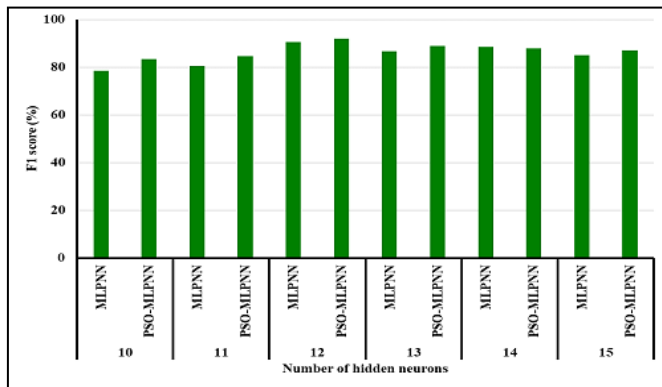
(a)



(b)

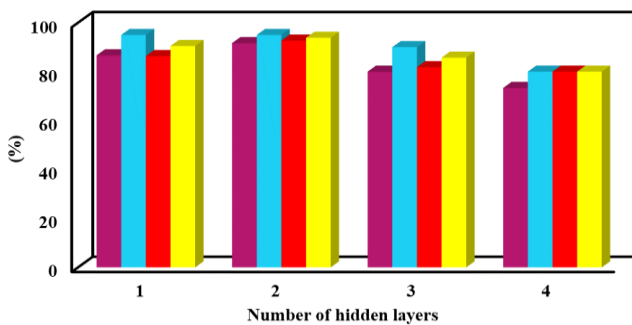


(c)

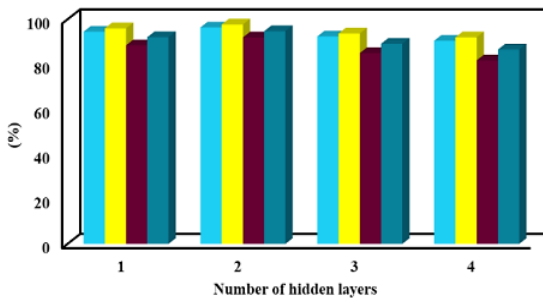


(d)

**Figure 3:** Performance assessment in terms of (a) accuracy, (b) recall, (c) precision, and (d) F1-score



(a) MLPNN



(b) PSO-MLPNN

**Figure 4:** Effectiveness comparison for varying number of hidden layers

### 4.2.3. Experiment 3

Based on the results obtained from the first and second experiments, the hidden layers and hidden neurons were set to 2 and 12, respectively. In the third scenario, the effectiveness of the MLPNN and PSO-MLPNN was analyzed by varying the number of training and test samples. The training samples ranged from 50% to 90%. The performance of the developed system for different training and testing data proportions is tabulated in *table 5*. It clearly demonstrates that the effectiveness of the developed system improved as the number of training samples increased from 50% to 80%. For the 50% testing data, the MLPNN and PSO-MLPNN achieved an accuracy of 85.23% and 90.29%. On the other hand, for the 10% test data, the MLPNN and PSO-MLPNN attained an accuracy of 90% and 93.14%, and F1-score values of, respectively. Notably, both the MLPNN and PSO-MLPNN produced outstanding results with 80% training and 20% testing data, reaching a higher accuracy of 91.67% and 96.38%, recall of 95% and 97.71%, and F1-score of, 93.83% and 94.74%, respectively. The empirical findings confirm that the developed system with a topology of 8-12-12-3 outperformed systems with other topologies, such as 8-12-3, 8-12-12-3, and 8-12-12-12-3. *Figure 5* graphically compares the effectiveness of the MLPNN and PSO-MLPNN for dissimilar numbers of test data.

The proposed PSO-MLPNN system provided improved results compared to the standard MLPNN. This improvement was evident as the system achieved higher values across all metrics assessed. The enhanced outcomes of the 8-12-12-3 topology can be attributed to the precise fine-tuning of the parameters of MLPNN using PSO. The superior results observed with the 8-12-12-3 topology can be directly linked to the optimization of MLPNN parameters utilizing the application of the PSO algorithm. The precision in fine-tuning the MLPNN parameters using PSO notably contributed to the system's enhanced performance and overall effectiveness.

**Table 5: Performance comparison between MLPNN and PSO-MLPNN for different numbers of training and testing samples**

Data ratio (%)	Models	Accuracy (%)	Recall (%)	Precision (%)	F1 score (%)
50:50	MLPNN	85.23	88.89	88.89	88.89
	PSO-MLPNN	90.29	92	81.31	86.33
60:40	MLPNN	86.67	91.67	88.71	90.16
	PSO-MLPNN	92.19	93.71	84.54	88.89
70:30	MLPNN	88.24	91.14	91.14	91.14
	PSO-MLPNN	94.67	96.57	88.48	92.35
80:20	MLPNN	91.67	95	92.68	93.83
	PSO-MLPNN	96.38	97.71	91.94	94.74
90:10	MLPNN	90	95	90.48	92.68
	PSO-MLPNN	93.14	95.43	85.64	90.27

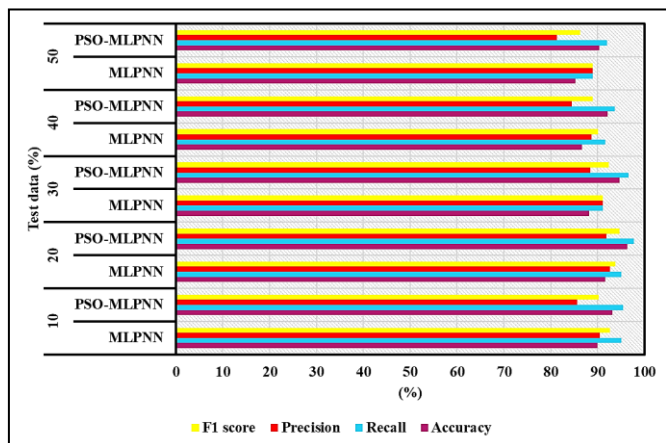


Figure 5: Effectiveness comparison for varying numbers of training and testing data

To further display its effectiveness, the performance of the proposed system, PSO-MLPNN is compared against two methods, namely NN [8] and mixed integer programming [11]. A comparative evaluation between the PSO-MLPNN and earlier approaches is given in table 6. From table 6, it is quite clear that the proposed method outperformed other methods notably because of the integration of PSO for optimization purposes.

Table 6: Performance comparison with earlier methods

Contributors	Method	Accuracy (%)
Brishty et al. [8]	NN	87.38
Ansari et al. [11]	Mixed integer programming	85.41
Proposed method	PSO-MLPNN	96.38

## 5. CONCLUSION

In this study, a novel framework for ink selection in printing applications has been presented. The system was designed using PSO and MLPNN. Initially, input data were gathered and then normalized using the min-max method. An MLPNN was designed and trained using the PSO and LM algorithms. The effectiveness of the proposed system was evaluated by altering the number of hidden neurons, hidden layers, as well as the training and testing data. The experimental results highlighted that the PSO-MLPNN with an architecture of 8-12-12-3 yielded superior results. However, the main constraint of this system pertains to the limited sample size used for analysis. For future investigations, deep learning models will be explored to enhance the ink selection process in printing applications. Other metaheuristic algorithms will also be taken into consideration to improve optimization and drive further advancements in results.

## REFERENCES

[1] Report, Flexible, printed and thin film batteries 2019-2029. IDTechfx.  
 [2] Lv, J., Thangavel, G. and Lee, P.S. 2023 Reliability of printed stretchable electronics based on nano/micro materials for practical applications. *Nanoscale*, 15(2): 434-449.

[3] Matsuhisa, N., Kaltenbrunner, M., Yokota, T., Jinno, H., Kuribara, K., Sekitani, T. and Someya, T. 2015 Printable elastic conductors with a high conductivity for electronic textile applications. *Nature Communications*, 6(1).  
 [4] Huang, X., Leng, T., Zhang, X., Chen, J. C., Chang, K. H., Geim, A. K., Novoselov, K. S. and Hu, Z. 2015 Binder-free highly conductive graphene laminate for low cost printed radio frequency applications. *Applied Physics Letters*, 106(20).  
 [5] Li, S., Peele, B. N., Larson, C. M., Zhao, H. and Shepherd, R. F. 2016 A Stretchable Multicolor Display and Touch Interface Using Photopatterning and Transfer Printing. *Advanced Materials*, 28(44): 9770-9775.  
 [6] Yao, X., Moon, S. K. and Bi, G. 2017 A hybrid machine learning approach for additive manufacturing design feature recommendation. *Rapid Prototyping Journal*, 23(6): 983-997.  
 [7] Babu, S. S., Mourad, A.-H. I., Harib, K. H. and Vijayavenkataraman, S. 2022 Recent developments in the application of machine-learning towards accelerated predictive multiscale design and additive manufacturing. *Virtual and Physical Prototyping*, 18(1).  
 [8] Brishty, F. P., Urner, R. and Grau, G. 2022 Machine learning based data driven inkjet printed electronics: jetting prediction for novel inks. *Flexible and Printed Electronics*, 7(1): 015009.  
 [9] Vahabli, E. and Rahmati, S. 2016 Application of an RBF neural network for FDM parts' surface roughness prediction for enhancing surface quality. *International Journal of Precision Engineering and Manufacturing*, 17(12): 1589-1603.  
 [10] Eberhart, R. and Kennedy, J. 1995 A new optimizer using particle swarm theory. *Proceedings of the Sixth International Symposium on Micro Machine and Human Science*. MHS'95.  
 [11] Ansari, N., Alizadeh-Mousavi, O., Seidel, H.-P. and Babaei, V. 2020 Mixed integer ink selection for spectral reproduction. *ACM Transactions on Graphics*, 39(6): 1-16.  
 [12] Nagasawa, K., Yoshii, J., Yamamoto, S., Arai, W., Kaneko, S., Hirai, K. and Tsumura, N. 2021 Prediction of the layered ink layout for 3D printers considering a desired skin color and line spread function. *Optical Review*, 28(4): 449-461.  
 [13] Wu, D. and Xu, C. 2018 Predictive Modeling of Droplet Formation Processes in Inkjet-Based Bioprinting. *Journal of Manufacturing Science and Engineering*, 140(10).  
 [14] V.K.R.Rama, V.A.Korada, P.S. Karthik and S.P. Singh 2015 Conductive silver inks and their applications in printed and flexible electronics. *RSC Advances*, 5(95): 77760-77790.  
 [15] Jansson, E., Lyytikäinen, J., Tanninen, P., Eiroma, K., Leminen, V., Immonen, K. and Hakola, L. 2022 Suitability of Paper-Based Substrates for Printed Electronics. *Materials*, 15(3): 957.  
 [16] Gupta, I., Choudary, M., Gnanasambanthan, G.H. and Maji, D. 2023 Optimization of microstructure patterning for flexible electronics application. *International Journal of Electrical and Electronics Research*, 11(3): 738-742.  
 [17] Anjani kumar, V. and Reddy, M.D. 2023 Fuzzy and PSO tuned PI controlled based SAPF harmonic mitigation. *International Journal of Electrical and Electronics Research*, 11(1): 119-125.  
 [18] Lavate, S.H. and Srivastava, P.K. 2023 A hybrid feature selection approach based on random forest and particle swarm optimization for IoT network traffic analysis. *International Journal of Electrical and Electronics Research*, 11(2): 568-574.



© 2023 by Alagusundari Narayanan & Dr. Sivakumari Subramania Pillai. Submitted for possible open access publication under the terms and conditions of the Creative Commons Attribution (CC BY) license (<http://creativecommons.org/licenses/by/4.0/>).